Testing of dye sensitized TiO$_2$ solar cells II: Theoretical voltage output and photoluminescence efficiencies

Greg Smestad

Paul Scherrer Institute, Laboratory for Energy and Process Technology, CH-5232 Villigen-PSI, Switzerland

(Received 1 September 1993; in revised form 21 December 1993)

Abstract

Detailed balance calculations have been applied to dye sensitized TiO$_2$ solar cells in order to obtain an upper limit for the solar conversion efficiency of the finished cell given the particular optical absorption and the luminescence efficiency, or fluorescence yield, of the dye. While these models do not predict the actual efficiency of the device they may serve as a guide for the reporting of actual open-circuit voltages and solar conversion efficiencies. The results of the analysis indicate that cells of at least 10% conversion efficiency with voltages of over 1 V are possible with Ru trinuclear complexes at AM 1.5.

1. Background: losses and ultimate efficiencies of quantum converters

Detailed balance calculations have long been used to obtain the ultimate efficiencies of solid state solar cells [1–6]. Originally pioneered by Shockley and Queisser [5] and extended to photochemical systems by Ross [6], these techniques consider the balance between the photon flux absorbed and the radiative and non-radiative recombination in the device. This is possible due to the knowledge of the theoretical spectral output of the radiative emission [7]. Band and Heller have experimentally demonstrated that predictions of this light output can be made for dye molecules as well as for semiconductors [8]. This point was also emphasized by Archer and Bolton [9] who applied these techniques to determine the radiative lifetimes of Si, CdS, GaAs and organic chromophores in order to study their performance as photochemical and photovoltaic solar energy converters. The application of these models to a photoconverter is possible due to four hypotheses:
(1) A thermalized two level (or band) system may describe the upper limit to conversion efficiency.

(2) Bodies which absorb light must also emit light described by the generalized Planck equation.

(3) Fluorescent emission is characterized by a non zero chemical potential, μ.

(4) Measured voltages are limited to this chemical potential, and, therefore, the efficiencies predicted by this analysis represent the upper limits to efficiencies in practical devices.

In the absence of non-radiative losses, the maximum efficiency for a single bandgap photovoltaic or photochemical conversion device, which accepts light from all angles, has been calculated to be 33% for the Air Mass 1.5 standard solar spectrum [1–3,6,10]. Noteworthy is that the maximum efficiency limit occurs within the range of bandgaps from 1.0–1.5 eV. Thus, materials in which the transition from low to high optical absorption occurs between 1200 nm to 800 nm are expected to produce devices with conversion efficiencies lower than 33%. This analysis can also be applied to concentrated sunlight or other standard spectra with comparable results [2]. Although these techniques are not widely used by those researching new photoconversion materials, they do represent a method for easily estimating the upper limit for the conversion efficiency and open-circuit voltages in practical systems. These models have been expanded to consider the actual shape of optical absorption spectra of the light absorber as well as the actual radiative and non-radiative recombination in the starting materials used for light absorption [4,6]. These limits thus represent a less idealized limit for the finished device. Specifically, they have been applied to silicon solar cells and even to photosynthesis found in nature [4–10]. In the case of silicon, losses due to non-radiative recombination such as Auger recombination limit the detailed balance AM 1.5 efficiency to approximately 29% and the voltage to approximately 0.77 V [4,10]. In the case of photosynthesis, excellent agreement was found between actual and expected energy levels and fluorescence yields [6]. In this paper, each of the above four hypotheses will be examined with regards to its relevance to dye sensitized solar cells [11]. Detailed balance calculations will be applied to Ru trinuclear dye sensitized TiO_2 solar cells and discussed in the light of experimental efficiency, voltage, photoluminescence, and $I–V$ curve results.

2. Application of detailed balance to sensitized solar cells

2.1. Application of a two level model to sensitized solar cells

Fig. 1 shows the energy band diagram of a dye sensitized solar cell. Light excites an electron in the dye layer to an excited energy state. This electron is rapidly transferred into an injecting energy state, is injected into the TiO_2, and is rapidly thermalized to the lowest level of the TiO_2 conduction band. Above this lowest conduction band level lies a continuum of states. The ground state of the dye is a singlet state, while the injecting level has been found to be a triplet state [12]. The electron injected into the TiO_2 particle eventually migrates to the SnO_2/back contact interface, is collected, and flows through the external load, producing
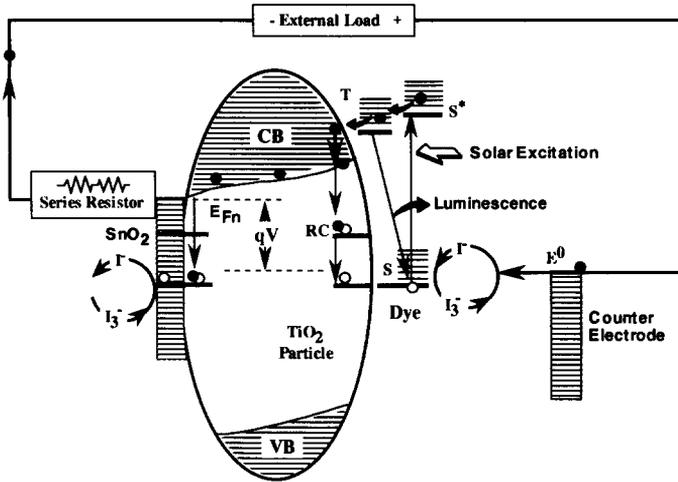
Fig. 1. Energy band diagram for loss mechanisms for the dye solar cell. Loss mechanisms include luminescent emission from the dye, series resistance of the glass and electrolyte (shown as the resistor at left), non-radiative recombination through defects (RC), and reaction of the iodine or triiodide with the TiO_2 before transfer of the electron to the counter electrode.

work. The oxidized dye is reduced by the iodide to form iodine or triiodide, which must diffuse through the pores of the electrode to itself become reduced at the counter electrode by the electron flowing though the external load. If the voltage is V, qV is the difference between the TiO_2 Fermi level, E_{Fn}, and the redox couple potential energy, E^0. The electron flow (or current) produced has been found to be approximately equal to the number of photo- excited electrons or absorbed photon flux [11].

How should one view the sensitized solar cell in relationship to conventional homojunction and heterojunction single crystal and thin film solar cells? Since dissimilar materials are used, i.e., TiO_2 and Ru dye, the homojunction analogy is not applicable. Much like a CdS–CdTe or $CdS–Cu_{1-x}S$ heterojunction solar cells, the dye sensitized cell is comprised of a large bandgap window layer, the TiO_2 or CdS, and the primary light absorber, the CdTe or Ru dye. Light can be absorbed by the TiO_2 if it is of wavelengths shorter than 375 nm, and by the dye if it is shorter than about 750 nm. Absorption by TiO_2 is not desired since the hole produced at the TiO_2 dye interface may photoxidize the dye. Due to it's large bandgap, the low solar flux value for UV photons, and the light absorption by the dye, the TiO_2 valence band, VB, does not participate significantly in the conversion process. One might also view the dye sensitized cell as a cousin of the a : Si PIN cell. In the PIN cell, the absorber is a thin insulating, or I, layer sandwiched between a layer with a high work function, such as the P doped layer, and a lower work function, such as the N type layer. Since the I-layer mobility is small, this configuration allows for rapid charge carrier separation and collection. In the dye sensitized cell, these "PIN" layers are: the redox couple, dye, and TiO_2 CB,

respectively. The analogy between the cell and the electron donor-Chlorophyl-electron acceptor configuration found in natural photosynthesis has previously been made by Graetzel [11]. The configuration used by Graetzel, with it's large optical pathlength, allows the use of low mobility materials, such as organic dyes, which otherwise [18] would exhibit low current collection efficiencies.

Even in the ideal case, where the redox level, E_0, is located at the dye ground level, this system is comprised of at least four levels; the TiO_2 conduction band, CB, the dye ground and injecting states, S and T, and the excited singlet state, S*, which quickly thermalizes and transfers the electron to the longer lived triplet state, T. The first hypothesis of the model would have one apply a two level model to this multilevel system. From the optical absorption spectrum of the dye, one observes a very weak absorption near the luminescence peak of the trinuclear dye (i.e., near 725 nm) [11,12]. As in the case of silicon, the luminescence is observed in a region where the optical absorption is rapidly decreasing [4,13]. At shorter wavelengths, the light is strongly re-absorbed and thus is only observed at longer wavelengths. One concludes from microscopic reversibility that there must be some weak absorption which can be attributed to singlet to triplet transitions which reverse during fluorescent emission. These transitions are expected to be weak due to the need of a change of spin of the electron. Due to this S–T absorption, one may consider the optical transitions as if they occurred from a two level, or band, system which possessed the same optical absorption as is measured for the dye. As will be further discussed in Section 2.3., detailed balance calculations do not require a detailed knowledge of the nature of the absorption and emission. One only needs to know the measured fraction of the incident light which produces excited states. In this paper, this quantum absorptivity [4] will simply be call the absorptivity. The above arguments would leave us with three levels; the TiO_2 CB, S and T. One might also consider that the electrons which are injected into the TiO_2 could, in principle be reverse injected back to the excited state of the dye. Granted that the rate constant for injection may be very large [11], and so this back reaction would be very small. However, no reaction occurs entirely in the forward direction and so the above conceptualization is reasonable. This will be expressed mathematically in Section 2.4.

In addition to the energy levels previously mentioned, recombination centers, RC, may be present at the TiO_2-dye interface which allow the excited electrons to decay non-radiatively without producing work (see Fig. 1). If one includes the recombination centers, one should model at least a four level system to be exact. One may still, however, gain insight from a two level system with recombination centers if one simply considers the *effect* of these defects on the ratio of radiative to non-radiative recombination without considering their location in the energy band diagram [4,6]. In this approach, as will be discussed in Section 2.4., the details of the location of the levels involved in absorption, recombination, and emission may be unknown, but their effect on these processes is known. In the sections that follow, the two level system represented by the dye will be viewed as a photochemical "pump" which transfers electrons from the iodide/triiodide redox couple to the third state represented by the conduction band of, or defect levels in, the titanium dioxide.

2.2. Luminescence and chemical potential

All materials which absorb light emit light. If this were not true, absorption of energy could result in an increase of absorber temperature above that of the source, in violation of the second law of thermodynamics [1,3]. If the emitted light from a solar converter is strictly black body work can be extracted *indirectly* by using a Carnot engine and by allowing the temperature of the converter to increase above the ambient temperature. In this case, the chemical potential of the absorber has not changed, but work can be extracted from the temperature difference. If direct conversion is required, as in photovoltaics or photochemistry, the free energy, μ, of the absorber must change. Fig. 2 shows the thought experiment [3] used to derive the relationship between voltage output and the luminescent emission in a general photoconverter. Consider a system in which a photoconverter (shown at the right) is coupled through a selective bandpass filter to black body emitter at temperature T_S. Both converter and source are housed in a perfectly reflecting cavity so that the only exchange of radiation takes place through the filter. This filter is perfectly reflecting for all photons except those in a narrow band centered on energy $e = h\nu$. Photons emitted in this band by the source, or by the converter, pass through the filter without losses. The photons may be absorbed by the photoconverter which is connected to a thermal reservoir of temperature T_0. Absorption of light produces excited electrons in the upper energy level, which may decay producing luminescent light, may be collected to
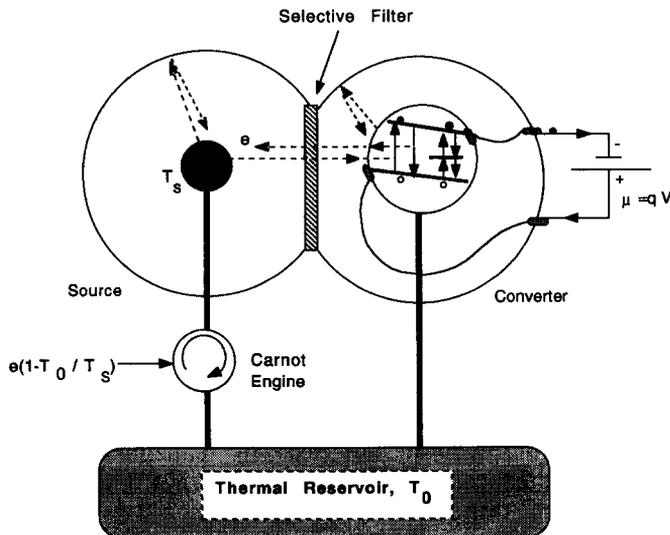
Fig. 2. Thought experiment used to determine the relationship between luminescent emission and photoconverter voltage. In the ideal case, the energy delivered to maintain the blackbody source at temperature T_S is equal to the chemical potential of the excited electrons, or $e(1 - T_0 / T_S) = qV$.

produce work, or may fall into intermediate trap or defect energy levels. The electrical work produced charges an ideal battery, or capacitor, at a voltage of $V = \mu/q$. In order for the temperature to remain at T_S, the energy loss from the source requires replacement via a heat pump connected to the thermal reservoir. This reversible Carnot engine delivers the necessary heat to the source, but requires an energy input of $e(1 - T_0/T_S)$. In addition, the battery provides the energy for the converter via the (shaded) electrical contacts to produce a photon travelling back to the source. When zero net electrical current flows, an equilibrium is set up such that an equal number of photons travel in both directions through the filter. In this paper, the various fluxes (i.e., the number of particles per unit area per unit time) will be given the symbol I, with the subscript indicating the origin or nature of the flow, and q is the elemental charge. We now consider the first level complexity which can be added to describe real materials. If an electron falls into an energy level between the upper and lower states, or is excited to this level via the absorption of light, additional photons are required to excite the electron so that it may be collected. The chemical potential of the electron in the intermediate state may be greater than that of the ground state but less than that of the final excited state. A given photon of energy e, therefore, contributes a chemical potential μ/A to the total process. In the ideal case, these intermediate levels are not present, each photon contributes equally to the chemical potential, and $A = 1$. In another ideal case, explored by Würfel [7], a defect level located half way between the upper and lower levels produces a two step process which results in an A value near 2. The flux emitted by the source, I_{BB}, is given by the well known Planck equation [1–3]

$$I_{BB} = \int_0^\infty \pi L_{Lum}(e,T_s)\,\mathrm{d}e = \pi \int_0^\infty \frac{2n^2}{h^3 c^2} \frac{e^2 \mathrm{d}e}{\exp\dfrac{e}{kT_s} - 1}, \tag{1a}$$

where L_{Lum} is the emitted radiance, h is Planck's constant, c is the velocity of light and n is the index of refraction in which the light is propagating. If the walls of the source container are transparent to some extent, an effective radiation temperature, T_r, replaces T_s [3]. From conservation of energy, we know from Fig. 2 that $\mu/A = e(1 - T_0/T_S)$ at equilibrium. We, therefore, obtain

$$(e - \mu/A)/kT_0 = e/kT_s. \tag{1b}$$

One may now connect the luminescent radiation emitted by the photoconverter, I_{0R}, at ambient temperature to the chemical potential of the excited state by recalling that $I_{BB} = I_{0R}$ at equilibrium. The resulting "generalized" Planck equation may be used for non-equilibrium cases by realizing that μ represents the maximum obtainable chemical potential, or free energy [3]. If the photoconverter is

---

Fig. 3. (a) Predicted luminescent emission spectra for 10^{-4} M Rhodamine 6G dye in dry ethanol, (b) measured optical absorption and predicted luminescence from a 10^{-4} M Ru trinuclear dye solution in ethanol, (c) measured IPCE and predicted luminescence from a finished Ru trinuclear dye cell.
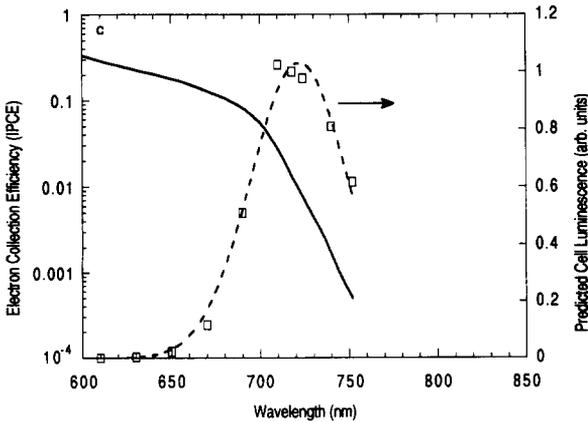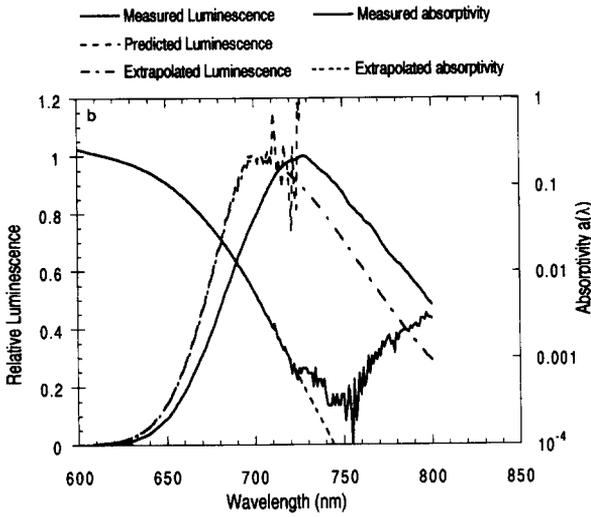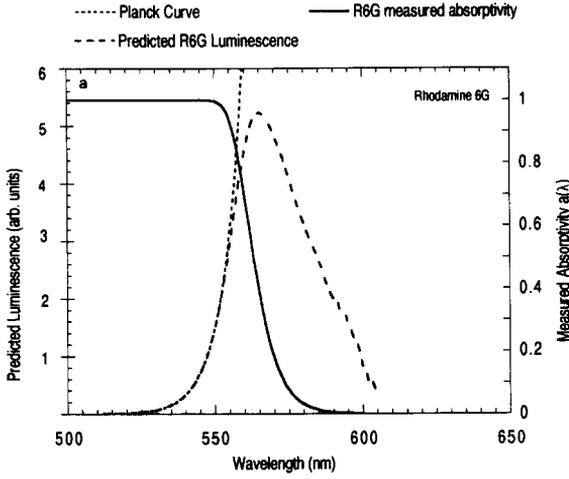
non-ideal in it's emission, an emissivity, $1 > \epsilon(e) > 0$, may be used such that $\epsilon(e)L_{\text{Lum}}$ replaces L_{Lum}. The relationship between the emissivity, the absorptivity and optical absorption will be discussed in the next section. The flux radiated by the converter when the source is switched off is I_0. It is obtained from Eq. (1b) by setting the chemical potential equal to zero and using this in Eq. (1a) [4]. Note that from Eqs. (1a) and (1b), $I_{0R} \sim I_0 \exp(\mu/kT_0)$. This relationship will be used in Section 2.4 to describe the maximum voltages and photoluminescence efficiencies expected for the dye TiO_2 cell.

2.3. Absorptivity and emissivity of dye sensitized cells

In order to apply detailed balance models to real materials, the emissivity of the attached dye must be known. There are two methods which can be used. If the emission of the cell can be directly measured, as is done for silicon solar cells [4,7,13], the emissivity can be inferred from Eq. (1). Luminescence was indeed observed from the dye in the solution [12] before attachment to the TiO_2. This luminescence is observed from the Ru trinuclear dye in an ethanol solution, but was not observed from a finished cell or from a dye coated TiO_2 film alone. As will be discussed shortly, the absence of detectable luminescence may point to fast electron injection into the TiO_2 and also to the presence of recombination centers, RC, or surface states within the forbidden band of the TiO_2. One can, therefore, not measure the emissivity directly. As is the case for many semiconductors [7,8] such as Silicon, the quantum emissivity, $\epsilon(e)$, is equal to the quantum absorptivity, $a(e)$. This permits the optical absorption of the dye in solution, or in the finished cell, to be used to estimate the emissivity. As demonstrated by Band and Heller [8], the absorption of a dye molecule such as Rhodamine can be used to predict the luminescence as shown in Fig. 3a. This technique was also applied to the Ru trinuclear dye, and the results are shown in Fig. 3b. In Fig. 3c, electron collection efficiency measured at short-circuit, IPCE [11], was used to estimate the shape of the luminescence curve. Both Figs. 3b and 3c seem to exhibit a peak output near the expected emission peak of the Ru dye. While the IPCE includes only the absorption which produces excited electrons, the optical absorption of the dye in solution also contains extraneous absorption due to impurities and other optical transitions in the dye. The IPCE thus better represents the absorptivity and emissivity. Note that unlike that from a silicon solar cell, the IPCE from the dye cell is directly related to the absorptivity since the electron injection efficiency is near 1. In silicon cells one must determine $a(e)$ from the known dependence between the current collection efficiency and the absorption coefficient and diffusion length [16]. Even if the actual dye cell emissivity is different from the measured absorptivity, the procedure may still be used since it is the order of magnitude for I_0 that is required for the calculations which follow. The flux I_0 is calculated from Fig. 3c to be 10^{-27} A/cm^2. The value for I_{sc}, the absorbed solar flux, can be estimated from the product of the IPCE, or from $a(e)$, and the number of AM 1.5 solar photons available at each wavelength [11,16]. If this is done for the Ru trinuclear dye, a qI_{sc} value of between 11 and 13 mA/cm^2 is obtained.

2.4. Recombination, detailed flux balance and current voltage characteristics

One may now determine the maximum open-circuit voltage of a photoconverter or the dye cell given it's emission. Shown in Fig. 4a is a generalized photochemical or photoelectrochemical system described by rate constants, k, and populations, or occupancies per unit area, P [6]. As shown in Fig. 1, the excited states produced from the absorption of light must decay in three ways: (1) radiatively, with the production of luminescent radiation, (2) non-radiatively, for example via defects, or (3) may produce collected electrons which dissipate their energy doing work as they flow through a load. The theoretical operational current through the load, qI, is found from the difference between the rate of creation of excited states produced by sunlight, I_{sc}, and the total (radiative *plus* non radiative) recombination current in the device, or

$$I = (I_{sc} - \sin\theta_S I_0) + (I_0 - I_{0R})/\Phi \cong I_{sc} - I_{0R}/\Phi, \tag{2a}$$
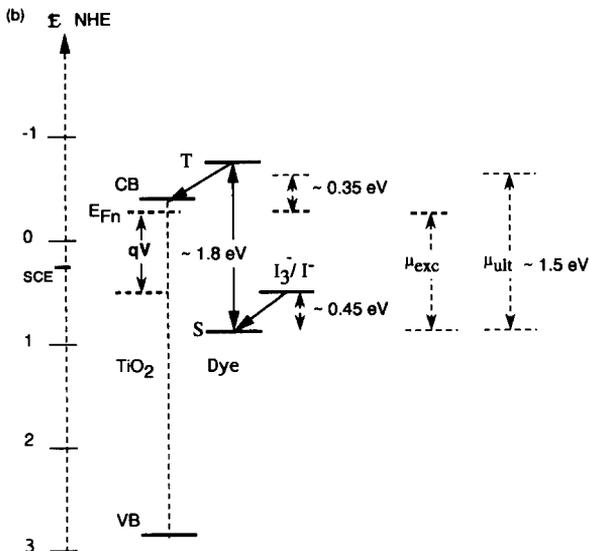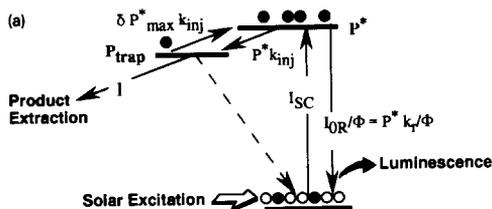
Fig. 4. Energy levels for: (a) a generalized photoconverter, and (b) the Ru trinuclear dye TiO₂ solar cell.

where Φ is the ratio of the radiative losses to the radiative plus non radiative recombination losses when the output current is zero. It is, therefore, equal to the open-circuit photoluminescence efficiency or fluorescence yield. When the non radiative losses are zero, the photoluminescence efficiency is unity, and all excitations decay radiatively at open-circuit. Luminescence is, therefore, a loss who's magnitude tells one about other losses in a device. The above relationship is essentially the same expression as previously described [4], with a small additional term, $\sin\theta_S\ I_0$, included to describe the ambient black body flux which arrives within the same solid angle, defined by the solar half angle θ_S, as the solar flux [14]. Using Eqs. (1a) and (1b), Eq. (2a) can be simply expanded to obtain an important expression identical to the diode equation used in semiconductor theory, solid state and photoelectrochemical solar cell I–V characteristics [3,4,10,16]. The reverse saturation current in this case is qI_0/Φ, where I_0/Φ is the blackbody flux that is radiated and absorbed by the dye in the dark. Even in the absence of an external light source, light is radiated by a light absorber in order to maintain equilibrium with the ambient thermal radiation field at temperature T_0. Since the value of I_0 is small for most materials of interest, the approximation in Eq. (2a) will be used for the rest of this discussion.

We may use Eq. (2), and a knowledge of the rate constants involved, to obtain a prediction of the luminescence efficiency of the photoconverter during operation. Under illumination, and at equilibrium, we know that the current extracted, qI, is zero and that the rate of upward transitions, which are induced by sunlight, must equal the total downward (recombination) rate (see Fig. 4a). If the excited state population is P^* in general, it is P^*_{max} when current or product extraction is zero. The equilibrium and non-equilibrium upward transition rate is therefore P^*_{max} $k_r/\Phi = I_{SC}$, where k_r is the radiative rate constant. The chemical potential of the excited state in the equilibrium condition is μ_{max}. Regarding the trap state, we know that there is no net transfer out of the trap, when it is in equilibrium with the excited state, and that the forward and reverse transfer rates are equal (see Fig. 4a). In other words,

$$P^*_{max} k_{inj} = P^{eq}_{trap} k_{rev},\tag{3}$$

where P^{eq}_{trap} is the equilibrium trap population and k_{inj} and k_{rev} are the forward transfer and reverse transfer rate constants, respectively. When it is in equilibrium with the excited state, the chemical potential of this trap is also μ_{max}. This potential is obtained from Eqs. (2a) and (1b) using the Wien approximation in Eq. (1a), and is given by

$$\mu_{max} \approx AkT_0\ln\frac{I_{sc}}{I_0} + AkT_0\ln\Phi,\tag{4}$$

where

$$\mu_{ult} = kT_0\ln\frac{I_{sc}}{I_0},\tag{5}$$
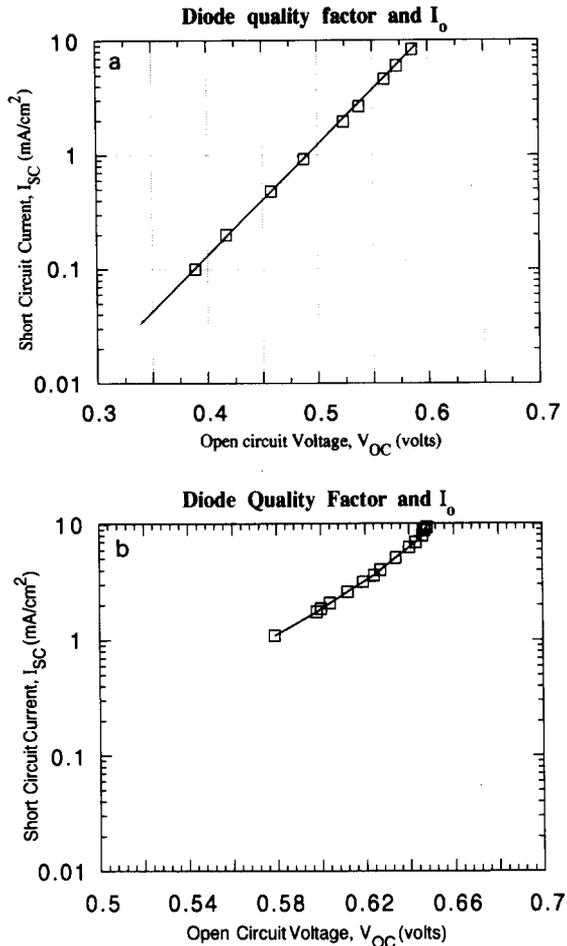
Fig. 5. Log(short-circuit current) versus open-circuit voltage for the Ru dye cell used to obtain the diode quality factor, A, and reverse saturation current [16]. Solute used for electrolyte: (a) Acetonitrile and ethylene carbonate 20/80 by volume, and for (b) solute was propylene carbonate and ethylene carbonate 50/50 by volume.

and μ_{ult} is the ultimate chemical potential obtained in the absence of all current extraction or non-radiative recombination. One may obtain an estimate for the factor A by using the short-circuit current, qI_{sc}, and open-circuit voltages, V_{oc}, values obtained for different illumination levels. Figs. 5a and 5b show the results from a measurement of the same trinuclear Ru dye solar cell. As predicted by Eq. (4), the log I_{sc} versus V_{oc} plot is a straight line. For the two different electrolytes used, the A and reverse saturation current (y-axis intercept) values are also different. These values are 1.6 and 10^{-9} A/cm^2 for Fig. 5a and 1.2 and 10^{-11} A/cm^2 for Fig. 5b. One would predict from Eq. (4) that the reverse saturation

current would give the value for I_0/Φ, but one must be careful. Given that the AM 1.5 I_{sc} value for the trinuclear Ru dye is 11–13 mA/cm^2 and the theoretical ideal dark current, I_0, is approximately 10^{-27} A/cm^2, one would predict that μ_{ult} is 1.5 V. One would predict from this I_0 value and the measured reverse saturation current that Φ is 10^{-16}, but this may not be the real value. As shown in Fig. 1, and as a dashed line in Fig. 4a, recombination centers and surface states may shunt some of the injected electrons back to the ground state of the dye. In addition, as shown at the left of Fig. 1, the iodine/triiodide may also back react at the SnO$_2$ or TiO$_2$ interface to regenerate the iodide instead of allowing for the production of the current. This shunting of the current means the cell is really never in open-circuit. The dye is either driving the load or, when the output voltage is zero, is driving electrons through these defects. It is for this reason that a very thin layer of TiO$_2$ may be useful [11] if it is deposited on the SnO$_2$ coated glass prior to the colloidal TiO$_2$, and on the TiO$_2$ colloids themselves, in order to decrease these defects and the back reaction. This treatment has experimentally been found to lower the measured A and reverse saturation currents. Since the above losses are incurred after the electron has been collected by the TiO$_2$, it is improper to assign them to the excited state of the dye. The cell should be viewed, instead, as a solar cell, represented by the dye, driving the uphill chemical reaction between the redox couple and trap (CB) state. In this sense, the Ru dye solar cell is unlike a Silicon cell, for which recombination and electron collection is inseparable and for which one can obtain Φ ($\Phi_{Si} = 10^{-3}$ to 10^{-4} [4]) from the reverse saturation current. The shunting current for dye sensitized cells should be subtracted from the right side of Eq. (2a) since it will lower the fill factors and operational currents [16]. In this case, the measured reverse saturation current is not I_0/Φ, but is related, instead, to the electrochemical black reaction. One must therefore look to non-equilibrium conditions to estimate the photoluminescence efficiency and chemical potential of the excited state of the dye.

Under non-equilibrium conditions, the population of the electrons in the trap will fall to some fraction, δ, of it's equilibrium value since current or product is being extracted from it. Combining this information with Eq. (3), we know that the reverse transfer rate is then given by $\delta P_{max}^* k_{inj}$. The chemical potential of the trap state will therefore decrease to some value

$$\mu_{trap} = \mu_{max} + kT\ln\delta \cong \mu_{ult} + kT\ln\delta\Phi. \tag{6}$$

The excited state population will also decrease, to some value P^*, when a current is extracted which means that the downward transfer rate resulting from radiative plus non radiative processes will be $P^* k_r/\Phi = I_{0R}/\Phi$. As before, we may balance the flow into and out of the excited state to obtain the extracted current from

$$I_{sc} - I_{0R}/\Phi = I = k_{inj}(P^* - \delta P_{max}^*). \tag{2b}$$

Since the photoluminescence efficiency under operation, Φ_{lum}, is the ratio of the radiative to the excitation or total recombination rate, we may use the

relationships deduced for I_{sc} and I_{0R} to obtain [6]

$$\Phi_{lum} = \frac{I_{0R}}{I_{sc}} = \frac{(k_r/k_{inj} + \delta\Phi)}{\left[1 + k_r/(\Phi k_{inj})\right]} . \tag{7a}$$

Using Eq. (6) for δ and assuming that the open-circuit photoluminescence efficiency is relatively large, and that k_{inj} is large compared to k_r, this equation may be approximated by

$$\Phi_{lum} \cong k_r/k_{inj} + \exp\frac{(\mu_{trap} - \mu_{ult})}{kT_0} . \tag{7b}$$

The chemical potential of the excited state, μ_{exc}, under operation, or for non-equilibrium conditions, is given by Eq. (4) if Φ_{lum} is substituted for Φ.

2.5. Theoretical maximum voltages and AM 1.5 conversion efficiencies

Fig. 4b shows the approximate energy band diagram for the Ru dye TiO$_2$ cell [11,12]. As a first estimate of the expected voltage from the dye cell, one may take the difference between the redox potential of iodide/triiodide and the TiO$_2$ E_{Fn} to obtain 0.7 V [11]. This is not, however, the maximum voltage one may obtain for this type of cell. In order to obtain μ_{exc} and Φ_{lum}, one now needs an estimate for the open-circuit photoluminescence, Φ. One estimate would be to take the Φ value of the Ru dye found in solution when it is not attached to the semiconductor. In this case, the dye is certainly not driving the reaction between the iodide and TiO$_2$ E_{Fn}, is at open-circuit and is not in contact with the surface states indicated by RC in Fig. 1. Given that the dye in solution has a luminescence efficiency of 5×10^{-3}, $\Phi \sim 10^{-3}$. One can then predict that μ_{max} is 1.3 eV. One can see from Fig. 4b, that μ_{trap}, represented by the TiO$_2$, is approximately 1 eV relative to the ground state of the dye. For a Φ value of 10^{-3} to 10^{-6}, a radiative rate constant of 10^4 s^{-1} and an injection rate constant of 10^{11} s^{-1} [11], Eqs. (7a) and (7b) yield a Φ_{lum} of approximately 10^{-6}, for a difference between the ultimate and trap chemical potential of 0.35 eV. This luminescence value is well below the limits of detection of most fluorescence detection equipment. If the photoluminescence efficiency of the finished cell is below 10^{-6} then Eq. (4) predicts that the voltage of the finished cell will be limited to $\mu_{exc} = 1.15$ eV even if an ideal redox couple is chosen with a redox potential near the ground state of the dye (see Fig. 4b). For the case of the iodide/triiodide redox couple, E^0 is about 0.45 V versus NHE. From the redox potential of the ground state of the dye, approximately 0.9 V (versus NHE), one should therefore expect to see no voltages higher than (1.15 − 0.45) = 0.7 V in practice. This is indeed the case for Ru dye cells, for which maximum (open-circuit) voltages rarely exceed 0.7 V [11]. For a fill factor of 0.7, qI_{sc} values of 12 mA/cm^2 and voltages in the range of 0.7–0.8, the AM 1.5 solar conversion efficiency is 6–7%, in agreement with measured devices. If no losses operated except luminescent emission, i.e., $\Phi = 1.0$, the conversion efficiency of an idealized cell would be approximately 30% [1–3].

There are two important conclusions one can draw from Eqs. (7a) and (7b). From Eq. (2a), and experiments, it is seen that as a current is drawn from the cell, the voltage decreases. This means that the TiO$_2$ E_{Fn} level at the SnO$_2$ interface is closer to the level of the redox couple and that $\mu_{ult} - \mu_{trap}$ increases. From Eqs. (7a) and (7b) this means that the luminescence is suppressed further. This is understandable, since the excited state population decreases in order to provide current output. The second conclusion is that if the injection rate constant is too large, *and* there is a large difference between the trap and ultimate chemical potentials, then the photoluminescence efficiency, Φ_{lum}, will decrease, as well as the chemical potential of the excited state of the dye, μ_{exc}. This will, in turn, lower the voltages that may be obtained from the dye TiO$_2$ cell. Hashimoto [17] has studied the kinetics of injection for a Ru(bpy) based dye adsorbed on various semiconductors and found that as the difference between the excited state energy level, P^*, and semiconductor CB is increased, the injection rate constant is also increased. Since for a particular dye there is a fixed value for μ_{ult} minus the excited state energy level, Hashimoto's observation would imply that as $\mu_{ult} - \mu_{trap}$ increases, so too will the injection rate constant (see Fig. 4b). This in turn would imply that faster injection may result in lower operational voltages in dye sensitized oxide based solar cells. One sees from this analysis that sacrificing some thermodynamic driving force results in rapid kinetics, and high IPCE [11].

As shown as the resistor in Fig. 1, there are also series resistance ohmic losses. In addition to the SnO$_2$ conductive glass coating, there is also the resistance caused by the slow diffusion of the redox couple to, and from, the counter electrode. In addition to these electrical losses, the conductive glass was found to have an integrated transmission, in the range of 400–900 nm, of 80%, and a reflection loss of 15%. These loss mechanisms will lower the actual efficiency of the dye cell when compared to the predictions presented in this paper.

2.6. Entropy, photoconversion and photochemistry

If one illuminates a solar cell or photochemical device with light of a given spectral distribution within it's absorption spectrum, luminescence will appear with a spectral distribution given by Eqs. (1a) and (1b). If one illuminates the same material with this luminescent spectral distribution, or if one applies a voltage, the original input spectrum will not re-appear. This is because the entropy creation, which was not directly calculated in Eq. (2), is non-zero as pointed out by De Vos [1], Parrot [14], and Würfel and Ruppel [15]. This entropy creation, ΔS, is obtained [14] from the difference between the net solar input power, P_{net}, and the output power generated by the solar converter, or

$$T_0 \Delta S = \eta_C P_{net} - P_{out}, \tag{8a}$$

where P_{out} is given by the product of q, the current in Eq. (2a) and the voltage. The factor η_C is the Carnot efficiency, $(1 - T_0/T_S)$, encountered in Section 2.2. The above equation is noteworthy, since it is immediately recognizable from the

thermodynamics of chemical reactions from the relationship between the free energy, ΔG, enthalpy, ΔH, and entropy,

$$\Delta G = \Delta H - T_0 \Delta S. \tag{8b}$$

In the absence of entropy generation, i.e., for a reversible converter, the photoconverter has a free energy generation rate, or power output, equal to the enthalpy input rate, which itself if equal to the Carnot efficiency times the net incoming solar power. This is understandable, since the Carnot efficiency is the maximum conversion efficiency for energy into work for an ideal reversible (and infinitely slow) system. A solar converter, be it a photosynthetic green leaf or a silicon solar cell, is thus seen to be merely a mediator for a chemical reaction between photons and electrons. The Ru dye, as stated previously, is seen as the mediator for the reaction between the redox system and the TiO_2.

3. Conclusions

In this paper, a thermodynamic based detailed balance model was applied to a Ru dye sensitized solar cell configuration and was found to be consistent with experimental observations which include the voltages and photoluminescence efficiencies. While the model does not consider the details involved in the absorption and recombination, it does apply a knowledge of the effects of these levels on the processes involved. From the optical absorption and photoluminescence efficiency, solar conversion efficiencies of 10%, and voltages of 1.1 V seem to be possible with the Ru Trinuclear dyes. Other dyes will give slightly different values depending on their photoluminescence values and optical absorption characteristics. It is remarkable that a device which is so easy to prepare functions in an analogous manner as does photosynthesis found in nature [6]. This may allow it, and the model presented, to be used in the teaching of electron transfer and photosynthesis. One concludes that detailed balance is enough to allow some *details* of dye sensitized solar cells and photoconversion to be understood.

4. References

[1] A. De Vos, Endoreversible Thermodynamics of Solar Energy Conversion (Oxford Science Publishers, Oxford, 1992).
[2] A. Luque and G. Araujo, Physical Limitations to Photovoltaic Conversion (Adam Hilger, New York, 1990).
[3] C. Winter, R. Sizman and L. Vant Hull, Solar Power Plants (Springer-Verlag, New York, 1991); H. Ries and A. McEvoy, J. Photochem. Photobio. A: Chem. 59 (1991) 11–18.
[4] G. Smestad and H. Ries, Sol. Energy Mater. Sol. Cells 25 (1992) 51; G. Smestad, Proc. SPIE Conf. on Energy Efficiency and Solar Energy Conversion XI, 18–22 May, 1992, Toulouse, France, SPIE, Bellingham, Washington 1992.
[5] W. Shockley and H.J. Queisser, J. Appl. Phys. 32 (1961) 510.
[6] R.T. Ross and T. Hsiao, J. Appl. Phys. 48 (1977) 4783; R.T. Ross and J.M. Collins, J. Appl. Phys. 51 (1980) 4504; R.T. Ross and M. Calvin, Biophys. J. 7 (1967) 595–614.

[7] K. Schick, E. Daub, S. Finkbeiner and P. Würfel, Appl Phys. A 54 (1992) 109; P. Würfel, Sol. Energy Mater. Sol. Cells 29 (1993) 403.

[8] Y.B. Band and D.F. Heller, Phys. Rev. A 38 (1988) 1885–95.

[9] M. Archer and J. Bolton, J. Phys. Chem. 94 (1990) 8028.

[10] T. Tiedje, E. Yablonovitch, G. Cody and B. Brooks, IEEE Trans. Elec. Dev. ED-31 (1984) 711.

[11] B. O'Regan and M. Graetzel, Nature 353 (1991) 737; M.K. Nazeeruddin, A. Kay and M. Graetzel, J. Am. Chem. Soc. 115 (1993) 6382; M. Graetzel, Comments Inorg. Chem. 12 (1991) 93–111; A. Mueller et al. (Eds.), Studies in Physical and Theoretical Chemistry, Vol. 78, Electron and Proton Transfer in Chemistry and Biology (Elsevier, Amsterdam, 1992).

[12] R. Amadelli, R. Argazzi, C. Bignozzi and F. Scandola, J. Am. Chem. Soc. 112 (1990) 7099; M. Nazeeruddin, P. Liska, J. Moser, N. Vlachopoulos and M. Graetzel, Heletica Chemica Acta 73 (1990) 1788.

[13] M.I. Gercenshtain and M.M. Koltun, Sol. Energy Mater. Sol. Cells 28 (1992) 1.

[14] J.E. Parrot, Sol. Energy Mater. Sol. Cells 25 (1992) 73.

[15] P. Würfel and W. Ruppel, J. Phys. C: Sol. State Phys. 18 (1985) 2987.

[16] C. Hu and R.M. White, Solar Cells From Basics to Advanced Systems (McGraw Hill, San Francisco, 1983); A. Fahrenbruch and R. Bube, Fundamental of Solar Cells (Academic Press, San Francisco, 1983).

[17] K. Hashimoto, M. Hiramoto. A. Lever and T. Sakata, J. Phys. Chem. 92 (1988) 1016.

[18] C.W. Tang, Appl. Phys. Lett. 48 (1986) 183; M. Hiramoto, H. Fujiwara and M. Yokoyama, Appl. Phys. Lett. 58 (1991) 1062.